Pharmacokinetic Analysis of Benzodiazepine Receptor Binding of [^{123}I]Iomazenil in Human Brain

Kiyomi Ito,[1,5] Toshimitsu Momose,[2] Hajime Kotaki,[3] Yoshiki Kojima,[2] Koujirou Yamamoto,[3] Masataka Katashima,[3] Yasufumi Sawada,[4] Yasuhito Sasaki,[2] and Tatsuji Iga[3]

Received November 12, 1996; accepted May 5, 1997

Purpose. The purpose of this study is to evaluate the central benzodiazepine (BZP) receptor binding of iomazenil (IMZ) by pharmacokinetic analysis and to establish a methodology for the diagnosis of CNS disorders with abnormalities in BZP receptor binding.

Methods. BZP receptor binding of IMZ was analyzed kinetically using plasma concentration-time profiles and dynamic single photon emission computed tomography (SPECT) data obtained after the intravenous administration of IMZ to patients with neuropsychiatric diseases. The analysis was based on a 3-compartmental model including the processes of both blood-brain barrier (BBB) transport and BZP receptor binding.

Results. Hydrolized metabolite of IMZ was detected in plasma, indicating the need for separation by HPLC. The BBB influx clearance and the receptor binding potential of IMZ in the medial temporal region was reduced in the epileptic patient.

Conclusions. Our findings suggest the possibility of detecting the epileptic focus by using our method.

KEY WORDS: iomazenil; SPECT; benzodiazepine receptor; human.

INTRODUCTION

[^{123}I]Iomazenil (IMZ), a specific antagonist at the central benzodiazepine (BZP) receptor, is a radioligand being developed for the imaging of human BZP receptors with single photon emission computed tomography (SPECT) (1–3). Previous studies with humans and nonhuman primates have demonstrated that IMZ has a high brain uptake and a distribution consistent with that of BZP receptors; this suggests that it may be useful in evaluating alterations in BZP receptor function (4–7).

It is widely accepted that the affinity and/or the density of BZP receptors in the central nervous system (CNS) can be altered in various disease states. For example, in epileptic patients, a significant reduction in BZP receptor binding in the epileptic focus has been reported by positron emission tomography (PET) studies using [^{11}C]flumazenil, which is another BZP antagonist with a chemical structure similar to IMZ (8–10).

The purpose of the present study is to evaluate the central BZP receptor binding of IMZ by pharmacokinetic analysis using plasma concentration-time profiles and dynamic SPECT data obtained after the intravenous administration of IMZ to patients with neuropsychiatric diseases and thus to establish a methodology for the diagnosis of CNS disorders with abnormalities in BZP receptor binding.

METHODS

SPECT Imaging

Six patients with neuropsychiatric diseases (1 with corticobasal degeneration, 2 with epilepsy, and 3 with spinocerebellar degeneration) participated in the study.

Iodine-123-iomazenil (IMZ) was supplied by Nihon Medi-Phisics Co., Ltd. (Hyogo, Japan). Each vial contained 167–222 MBq I-123. The specific activity was 2500 Ci/mmol and the radiochemical purity was greater than 95%.

This study was approved by the Institutional Review Board of Tokyo University Hospital. Each subject received 167–222 MBq of IMZ intravenously over 1 min in the antecubital vein. A catheter was inserted in the radial artery for blood sampling. Arterial blood samples were drawn manually at 15-sec intervals for the first 2 min and 2.5, 3, 3.5, 4, 4.5, 5, 7, 10, 20, 30, 45, 60, 80, 100, 120, and 180 min. SPECT data were acquired with a triple headed SPECT gammacamera system equipped with high-resolution fanbeam collimators and 159 kev + 10% of the photo window (GCA9300A, Toshiba). The transaxial resolution of this system was 7.5 mm full width at half maximum (FWHM). Scans were acquired continuously in a continuous rotating model (40 steps/120/60 sec) until 120 min postinjection. The acquisition times were 2 min for the first 15 scans and 5 min thereafter.

Images were reconstructed from photopeak counts (159 + 16 kev) with a Butterworth filter and were displayed on a 64 × 64 matrix (pixel size = 3.4 × 3.4 mm, slice thickness = 6.8 mm). Attenuation correction was not performed. Four transaxial slices were selected, the level of which were cerebellum, medial temporal (hippocampus), thalamus and centrum semiovale, respectively. Ten regions of interest (ROIs) were placed on the frontal cortex, occipital cortex, temporal cortex, parietal cortex, centrum semiovale (white matter), thalamus, basal ganglia, cerebellum, pons, and medial temporal region (hippocampus) for data analysis. The time courses of radioactivity in each region was calculated from 33 points of the dynamic SPECT data.

Measurement of Plasma IMZ Concentration

Plasma 500 μl was mixed with 1 ml of buffer solution (0.2 N Na_2HPO_4 adjusted to pH 10.5 with NaOH) in a centrifuge

[1] Department of Pharmaceutics, Faculty of Pharmaceutical Sciences, University of Tokyo, 7-3-1 Hongo, Bunkyo-ku, Tokyo 113, Japan.
[2] Department of Radiology, University of Tokyo Hospital, Faculty of Medicine, University of Tokyo, 7-3-1 Hongo, Bunkyo-ku, Tokyo 113, Japan.
[3] Department of Pharmacy, University of Tokyo Hospital, Faculty of Medicine, University of Tokyo, 7-3-1 Hongo, Bunkyo-ku, Tokyo 113, Japan.
[4] Faculty of Pharmaceutical Sciences, Kyushu University, 3-1-1 Maidashi, Higashi-ku, Fukuoka 812, Japan.
[5] To whom correspondence should be addressed.

ABBREVIATIONS: IMZ, [^{123}I]iomazenil; BZP, benzodiazepine; SPECT, single photon emission computed tomography; BBB, blood-brain barrier; CNS, central nervous system; PET, positron emission tomography; Cp, plasma IMZ concentration; τ, time to peak plasma concentration; n, the number of compartments; Xf, the amount of free and nonspecifically bound IMZ in brain; Xb, the amount of IMZ bound to the receptor; K_1, the influx clearance of IMZ from plasma to brain; k_2, the efflux rate constant from brain to plasma; k_3, the rate constant for receptor binding; k_4, the rate constant for receptor dissociation; F, cerebral blood flow; PS_1, intrinsic clearance for BBB permeability; kon, receptor association rate constant; koff, receptor dissociation rate constant; Bmax, receptor density; Vd, tissue water volume; BP, receptor binding potential; Kd, receptor dissociation constant.

0724-8741/97/0800-0999$12.50/0

tube. The samples were extracted with diethylether/dichloromethane (60/40; v/v) 5 ml for 30 sec on a Vortex mixer and then centrifuged for 5 min at 2000 g. 4 ml of the organic phase was transferred into another centrifuge tube and evaporated to dryness in a water bath at 40°C under a gentle stream of pure nitrogen. Finally, the residue was dissolved in 100 μl of the mobile phase and 20 μl was injected into the HPLC system. The column used was NUCLEOSIL 7 C18 (25 cm × 4.6 mm, 7 μ, Macherey-Nagel). The column temperature was set at 50°C. The mobile phase consisted of acetonitrile/0.3% NaH_2PO_4 (pH 4.0) (30/70; v/v) and the flow rate was 1.5 ml/min.

On the other hand, radioactivities in 0.3 ml each of the whole blood, plasma, and the organic phase after extraction were counted with a well counter.

Standard solutions for calibration were prepared by diluting the injectate solution with blank plasma. The extraction ratio was calculated to be 94.1–106.0% using the radioactivities in the standard solution and in the organic phase after extraction.

Analysis

Plasma IMZ concentration (Cp) was fitted to the following equations and parameters C and λ were obtained by the nonlinear least squares regression method (MULTI) (11).

During infusion ($t < \tau$):

$$Cp = \frac{1}{\tau} \cdot \sum_{i=1}^{n} \frac{C_i}{\lambda_i} \{1 - \exp(-\lambda_i \cdot t)\} \quad (1)$$

After infusion ($t \geqq \tau$):

$$Cp = \frac{1}{\tau} \cdot \sum_{i=1}^{n} \frac{C_i}{\lambda_i} \{\exp(\lambda_i \cdot t) - 1\} \exp(-\lambda_i \cdot t) \quad (2)$$

where τ represents the time to peak plasma concentration (about 1 min) and n is the number of compartments (2 or 3).

Figure 1 shows the 3-compartment model used for the analysis of the IMZ disposition in brain. Because greater than 90% of the radioactivity in the monkey brain was reported to be unchanged parent IMZ (2), the radioactivity measured by SPECT was assumed to be the sum of Xf (the amount of free and nonspecifically bound IMZ in the brain) and Xb (the amount of IMZ bound to the receptor). Using a plasma concentration profile (Eq. 1 and 2) as an input function, the radioactivity in the brain was fitted to the following equations (Eq. 3 and 4) and parameters K_1 (the influx clearance of IMZ from plasma to brain; ml/g/min), k_2 (the efflux rate constant from brain to plasma; min^{-1}), k_3 (the rate constant for receptor binding; min^{-1}), and k_4 (the rate constant for receptor dissociation; min^{-1}) were obtained by nonlinear least squares regression method (PCNONLIN; Statistical Consultants Inc, Lexington, KY).

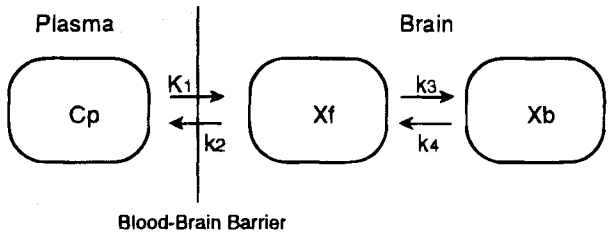

Fig. 1. Kinetic model used for the analysis of IMZ disposition in the brain. Cp is the plasma concentration of IMZ; Xf is the amount of free and nonspecifically bound IMZ in brain; Xb is the amount of IMZ bound to the receptor; K_1 is the influx clearance of IMZ from plasma to brain (ml/g/min); k_2 is the efflux rate constant from brain to plasma (min^{-1}); k_3 is the rate constant for receptor binding (min^{-1}); k_4 is the rate constant for receptor dissociation (min^{-1}).

$$\frac{dXf(t)}{dt} = K_1Cp(t) - (k_2 + k_3)Xf(t) + k_4Xb(t) \quad (3)$$

$$\frac{dXb(t)}{dt} = k_3Xf(t) - k_4Xb(t) \quad (4)$$

RESULTS

Figure 2 shows the time courses of plasma concentrations of IMZ and its hydrolized metabolite measured by HPLC. As shown in Fig. 2, the metabolite of IMZ appeared in plasma at a level almost equivalent to that of the parent IMZ. The pharmacokinetic parameters in Eq. 1 and 2 are summarized in Table I.

Figure 3 shows the time-activity curves in the various regions of brain after the intravenous administration of IMZ to patients No. 2 and 5. In both patients, IMZ showed rapid uptake into each brain region with peaks at 20–30 min post injection. High accumulation and slow elimination was observed in occipital, frontal, and temporal cortex. In basal ganglia and thalamus, the initial radioactivity was almost as high as that in cerebral cortex, which was followed by a relatively rapid washout. Furthermore, radioactivities in white matter and pons were low, indicating that the distribution pattern of the accumulation of IMZ in the brain is consistent with that of BZP receptor.

Patient No. 5 in Fig. 3 is an epileptic patient with focus in hippocampus. In this patient, radioactivities in the medial temporal region where hippocampus is included were considerably low compared with other regions investigated.

In Fig. 4, the influx clearance of IMZ through BBB (K_1) in the medial temporal region is compared among patients. A significantly low K_1 value was obtained in patient No. 5 who has epileptic focus in hippocampus, compared with other patients with normal hippocampus. Parameters for patient No. 3 could not be obtained because of the abnormal patterns of the time-activity curves probably due to the change in position during the SPECT study.

Figure 5 shows the parameters for the BZP receptor binding in the medial temporal region. While k_3 was reduced in patient No. 5, the interindividual variation in k_4 was not very large, resulting in a reduced value of binding potential (k_3/k_4) in patient No. 5.

DISCUSSION

The plasma concentration of IMZ declined 2- or 3-exponentially after intravenous administration to 6 patients with neuropsychiatric diseases (Fig. 2, Table I). As shown in Fig. 2, the plasma metabolite level was almost equivalent with that of the parent IMZ in some patients, indicating that IMZ and its metabolite have to be separated in the assay.

Using a plasma IMZ concentration profile as an input function, the time courses of regional radioactivity in the brain were fitted to a 3-compartment model (Fig. 1). As shown in

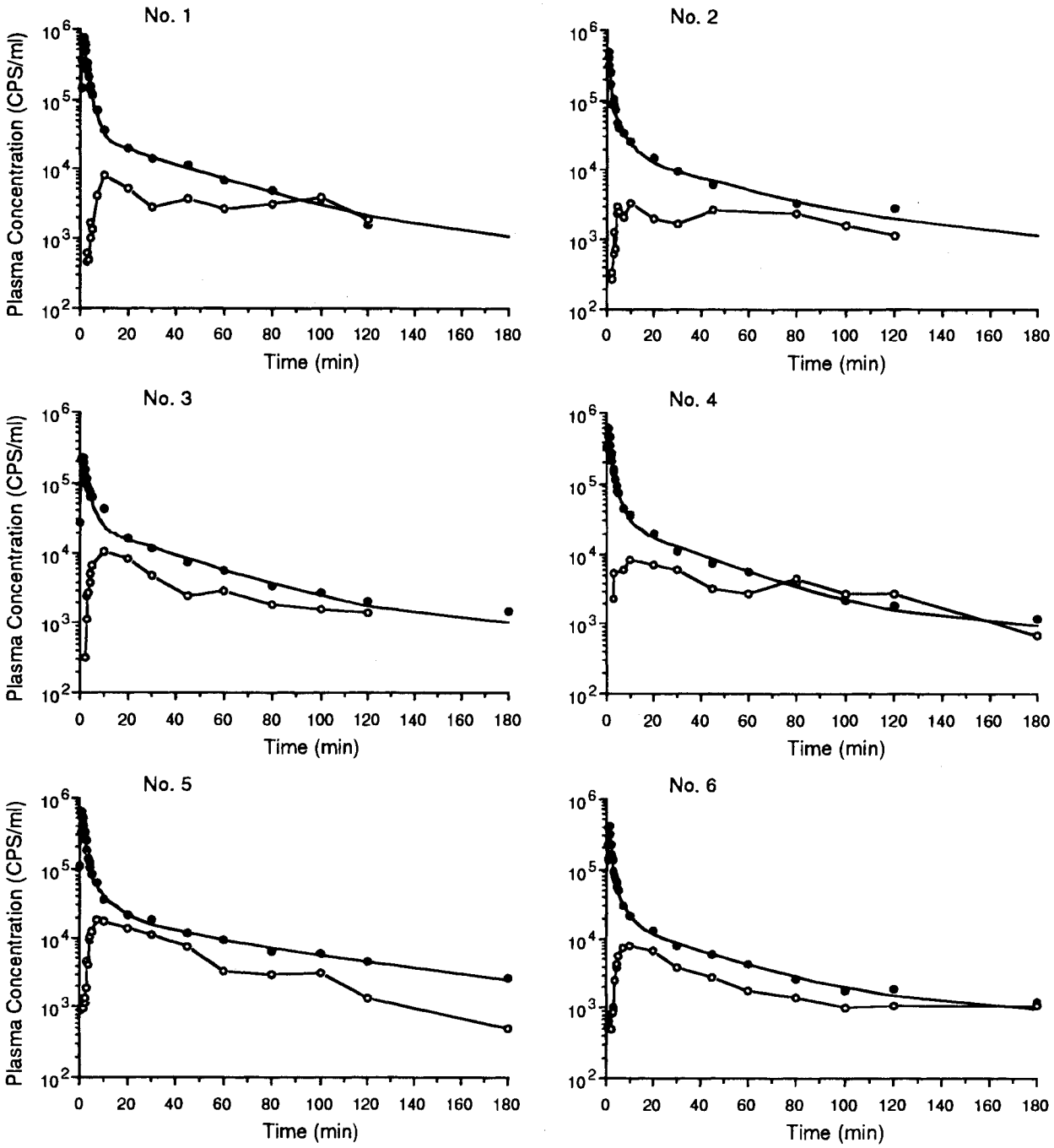

Fig. 2. Time courses of plasma concentrations of IMZ and its hydrolized metabolite after intravenous administration of IMZ. Closed circle: IMZ, Open circle: metabolite.

Fig. 4, the K_1 value in the medial temporal region, which includes hippocampus, was reduced by about 50% in the epileptic patient (No. 5) whose epileptic focus exists in hippocampus. K_1 is a hybrid parameter that consists of the cerebral blood flow (F) and the intrinsic clearance for BBB permeability (PS_1):

$$K_1 = F \cdot \{1 - \exp(-PS_1/F)\} \quad (5)$$

In patient No. 5, the cerebral blood flow has also been estimated to be reduced to about 50% of the normal value (unpublished observation in the PET study), suggesting that PS_1 of IMZ is also reduced by approximately 50%.

Furthermore, as shown in Fig. 5, the k_3/k_4 value in the medial temporal region was also reduced in patient No. 5. Values of k_3 and k_4 can be expressed as follows using kon (receptor association rate constant), koff (receptor dissociation rate constant), Bmax (receptor density), and Vd (tissue water volume):

$$k_3 = \frac{\text{kon} \cdot \text{Bmax}}{\text{Vd}} \quad (6)$$

$$k_4 = \text{koff} \quad (7)$$

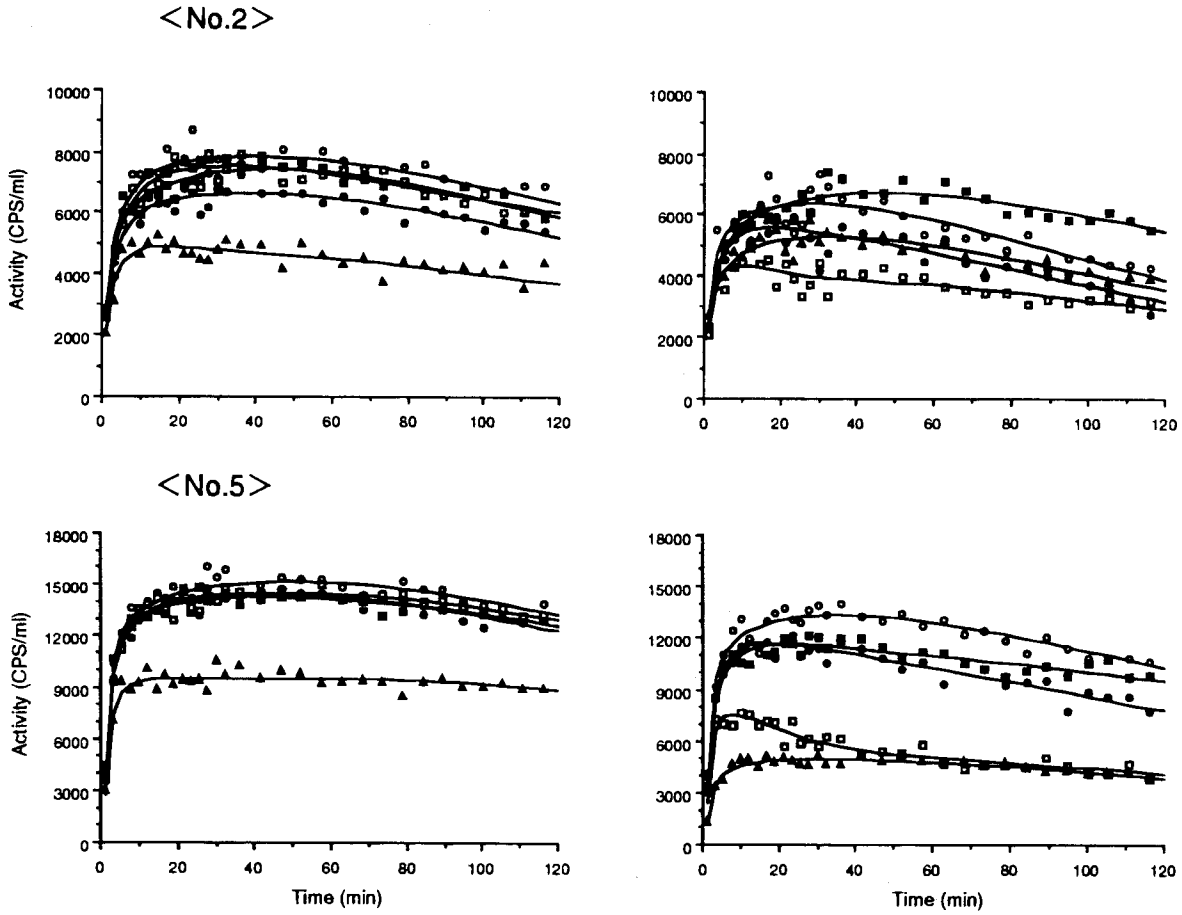

Fig. 3. Time-activity curves after the intravenous administration of IMZ to patients No. 2 and 5. Left panel: ● frontal cortex; ○ occipital cortex; ■ temporal cortex; □ parietal cortex; ▲ white matter. Right panel: ● thalamus; ○ basal ganglia; ■ cerebellum; □ pons; ▲ medial temporal region.

Equation 8 can be derived from Eqs. 6 and 7:

$$\frac{k_3}{k_4} = BP = \frac{Bmax}{Kd \cdot Vd} \tag{8}$$

where BP represents receptor binding potential and Kd (= koff/kon) is the receptor dissociation constant. It was indicated, therefore, that the density or the affinity of BZP receptor in the medial temporal region was reduced in patient No. 5. This result is consistent with previous findings of reduced BZP receptor density in epileptic focus (8–10), suggesting the possibility of detecting the epileptic focus by the present method.

Table I. Pharmacokinetic Parameters for IMZ

Patient	No. 1	No. 2	No. 3	No. 4	No. 5	No. 6
τ (min)	1.25	0.75	1	1	1	1.25
C_1 (CPS/ml)	32922	28564	9888	32658	27898	20216
λ_1 (min^{-1})	0.481	1.972	0.433	2.028	0.708	1.126
C_2 (CPS/ml)	1387	4209	1166	10874	3105	3964
λ_2 (min^{-1})	0.0267	0.2311	0.0274	0.3631	0.1257	0.2640
C_3 (CPS/ml)		774		1373	932	830
λ_3 (min^{-1})		0.02290		0.03053	0.01420	0.02798

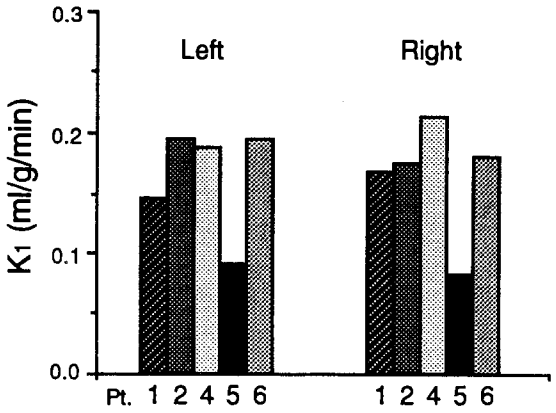

Fig. 4. Comparison of K_1 values in the medial temporal region among patients.

In conclusion, a significant amount of IMZ metabolite was detected in plasma after intravenous administration, indicating the need for separation by HPLC. Pharmacokinetic analysis allowed a quantitative evaluation of the processes of both BBB transport and BZP receptor binding. BBB influx clearance and the receptor binding potential of IMZ in the medial temporal

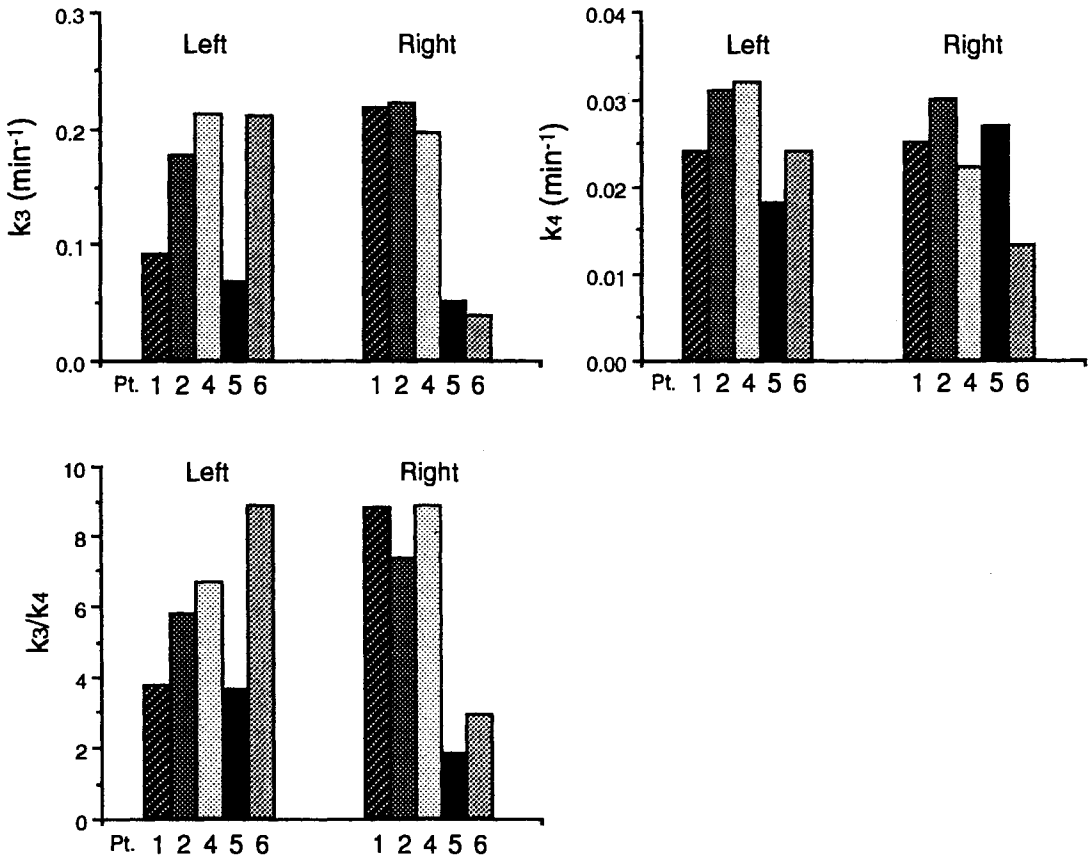

Fig. 5. Comparison of BZP receptor binding parameters in the medial temporal region among patients.

region was reduced in the epileptic patient, suggesting the usefulness of this pharmacokinetic analysis in the detection of the epileptic focus.

REFERENCES

1. H.-F. Beer, P. A. Blauenstein, P. H. Hasler, B. Delaloye, G. Riccabona, I. Bangerl, W. Hunkeler, E. P. Bonetti, L. Pieri, J. G. Richards, and P. A. Schubiger. *J. Nucl. Med.* **31**:1007–1014 (1990).
2. S. S. Zoghbi, R. M. Baldwin, J. P. Seibyl, M. S. Al-Tikriti, Y. Zea-Ponce, M. Laruelle, E. H. Sybirska, S. W. Woods, A. W. Goddard, R. T. Malison, R. Zimmerman, D. S. Charney, E. O. Smith, P. B. Hoffer, and R. B. Innis. *Nucl. Med. Biol.* **19**:881–888 (1992).
3. H. M. Dey, J. P. Seibyl, J. B. Stubbs, S. S. Zoghbi, R. M. Baldwin, E. O. Smith, I. G. Zubal, Y. Zea-Ponce, C. Olson, D. S. Charney, P. B. Hoffer, and R. B. Innis. *J. Nucl. Med.* **35**:399–404 (1994).
4. M. Laruelle, R. M. Baldwin, Z. Rattner, M. S. Al-Tikriti, Y. Zea-Ponce, S. S. Zoghbi, D. S. Charney, J. C. Price, J. J. Frost, P. B. Hoffer, and R. B. Innis. *J. Cereb. Blood Flow Metab.* **14**:439–452 (1994).
5. M. Laruelle, A. Abi-Dargham, M. S. Al-Tikriti, R. M. Baldwin, Y. Zea-Ponce, S. S. Zoghbi, D. S. Charney, P. B. Hoffer, and R. B. Innis. *J. Cereb. Blood Flow Metab.* **14**:453–465 (1994).
6. A. Abi-Dargham, M. Laruelle, J. Seibyl, Z. Rattner, R. M. Baldwin, S. S. Zoghbi, Y. Zea-Ponce, J. D. Bremner, T. M. Hyde, D. S. Charney, P. B. Hoffer, and R. B. Innis. *J. Nucl. Med.* **35**:228–238 (1994).
7. Y. Onishi, Y. Yonekura, T. Mukai, S. Nishizawa, F. Tanaka, H. Okazawa, K. Ishizu, T. Fujita, H. Shibasaki, and J. Konishi. *J. Nucl. Med.* **36**:1201–1210 (1995).
8. I. Savic, A. Persson, P. Roland, S. Pauli, G. Sedvall, and L. Widen. *Lancet* **2**:863–866 (1988).
9. H. Shinotoh, Y. Tateno, and K. Hirayama. *Rinsho-Shinkei* **28**:437–446 (1988).
10. T. R. Henry, K. A. Frey, J. C. Sackellares, S. Gilman, R. A. Koeppe, J. A. Brunberg, D. A. Ross, S. Berent, A. B. Young, and D. E. Kuhl. *Neurology* **43**:1998–2006 (1993).
11. K. Yamaoka, Y. Tanigawara, T. Nakagawa, and T. Uno. *J. Pharmacobio.-Dyn.* **4**:879–885 (1981).